

RESEARCH ARTICLE

Green Synthesis and Evaluation of Copper Oxide Nanoparticles using Fig Leaves and their Antifungal and Antibacterial Activities

Jenan Hussien Taha^{1*}, Nada Khudair Abbas², Azhar A. F. Al-Attraqchi³

¹Department of Physics, College of Science, University of Baghdad, Baghdad, Iraq

²Department of Biology, College of Science, University of Baghdad, Baghdad, Iraq

³Department of Microbiology, College of Medicine, University of Al-Nahrain, Baghdad, Iraq

Received: 27th June, 2020; Revised: 20th July, 2020; Accepted: 27th August, 2020; Available Online: 25th September, 2020

ABSTRACT

In this article, a simple new technique for the green synthesis of copper oxide nanoparticles (CuO NPs) using peroxidases oxidoreductases (POX) enzyme extracted from fig leaves for antifungal and antibacterial activities has been reported. Subsequently, a comprehensive investigation of the structural, optical, and morphological properties of the synthesized CuO NPs was elucidated, using X-ray diffraction (XRD), Fourier transform infrared spectroscopy (FT-IR), Electrodiagnostic (EDX), atomic force microscopy (AFM), and transmission electron microscopy (TEM) analysis techniques. Specifically, the resultant nanoparticles are spherical with a diameter ranging from 28–68. CuO NPs were further tested for their antifungal activity against *Candida* and *Aspergillus* species, while the antibacterial activity was screened in contradiction of pathogenic bacterial strains namely gram-positive *Staphylococcus aureus* and gram-negative *Asinobacterial* species. The present study reveals a convenient use of POX fig leaves extract as fuel, for the well-organized synthesis of CuO NPs via green synthesis technique to acquire considerably active antifungal and antibacterial materials.

Keywords: Antibacterial, Antifungal, Copper oxide nanoparticles, Peroxidases oxidoreductases.

International Journal of Drug Delivery Technology (2020); DOI: 10.25258/ijddt.10.3.13

How to cite this article: Taha JH, Abbas NK, Al-Attraqchi Azhar AF. Green synthesis and evaluation of copper oxide nanoparticles using fig leaves and their antifungal and antibacterial activities. International Journal of Drug Delivery Technology. 2020;10(3):378-382.

Source of support: Nil.

Conflict of interest: None

INTRODUCTION

CuO NPs, which are p-type semiconductor with an energy band gap of ~1.7 eV, have drawn a remarkable consideration due to their electrical, optical, and catalytic properties.^{1,2} CuO NPs are widely employed in a variety of applications, for instance, catalytic,³ sensors,^{4,5} gas sensors,⁶ solar energy,⁷ thermoelectric,^{8,9} and high-temperature superconductors.¹⁰ In addition, CuO NPs are extensively applied in the medical field as an antifungal, antimicrobial, and antibiotic agent, especially when combined with plastics, textiles, and coating.² Copper and other copper-based compounds have shown highly effective biocidal features, in which these properties, generally, can be employed in a number of health-related applications, pesticidal formulation in particular.¹¹ Therefore, a number of CuO NPs preparation methods for biomedical applications are available, viz., alkoxide based route,¹² sonochemical,⁷ microwave irradiations,¹³ electrochemical procedure,¹⁴ solid-state reaction technique,¹⁵ precipitation pyrolysis,¹⁶ and thermal decomposition of precursor.¹⁷ In general, the aforementioned chemical synthesis techniques result in the

occurrence of toxic chemicals that are absorbed onto the NPs' surface. These toxic chemicals can lead to dramatic negative effects in the medical application, biomedical in particular.² Recently, a new approach, namely green synthesis technique, has been established for the synthesis of metal oxide NPs which demonstrates low toxic presence. The green synthesis approach of metal oxide NPs is associated with the use of enzymes extracted from different plants as fuel; among these plants are lemongrass,¹⁸ alfalfa,¹⁹ *Euphorbia tirucalli*,²⁰ tamarinds,²¹ *Cinnamomum camphora*,²² etc.

POX, which is known as (EC.1.11.1.7), has drawn significant attention as a preferred eco-friendly and cost-effective green NPs synthesis agent.^{1,23} POX enzyme has attractive features, such as, catalyze redox reactions and electron transfer. Currently, POX enzyme is purified from different plants, such as, strawberries, wheat, potatoes, soybeans, dates, tomatoes, and apricots.²⁴ In this attempt, this study aims to demonstrate the synthesis of CuO NPs using the POX enzyme purified from fig leaves as a fuel. Continuously, the structural and morphological properties of the attained product (CuO NPs)

*Author for Correspondence: asjenan@gmail.com

are demonstrated in detail. Furthermore, using the agar well diffusion method, the synthesized CuO NPs were evaluated for antifungal activity using *Candida* and *Aspergillus* species alongside antibacterial activity by employing gram-positive *S. aureus* and gram-negative *Asinobacterial* species.

MATERIALS AND METHODS

Plant and Enzyme Extraction

Fresh leaves of fig have been obtained from Baghdad, Iraq, and thoroughly washed with distilled water at room temperature. Fifty grams of the washed leaves were shattered into small pieces and blended to form a homogeneous mixture along with 10 mm of sodium phosphate (pH 6).²⁵ The resultant mixture was subjected to centrifuge at 7,000 rpm for 10 minutes. The obtained supernatant was saturated with ammonium sulfate (60–80%) under a stirring rate of 500 rpm for 1-hour, for the purpose of enzyme purification. Consequently, the POX was obtained through centrifuging at 8,400 rpm for 30 minutes. The final precipitate was dissolved in 10 mm of sodium phosphate and incubated at 4°C for further use in CuO NPs synthesis.

Synthesis of CuO NPs

In a typical procedure, the reaction mixture was prepared by dissolving a particular amount (7, 10, and 15 mm) of hydrated copper dichloride ($\text{CuCl}_2 \cdot 2\text{H}_2\text{O}$, Sigma Aldrich) in 100 mL of deionized-distilled water (DDW) at room temperature, with stirring rate of 500 rpm for 10 minutes.¹ Concurrently, the purified peroxidase was poured into the solution and left for stirring for 4 hours, while the residual water was eliminated using an evaporator. The attained precipitate was subsequently washed with a multi-cycle centrifugation procedure. Finally, the synthesized CuO was post-baked at 70°C for 12 hours. Hereinafter, the CuO samples are denoted as 7, 10, and 15 mm, respectively.

Characterization

The structural properties were investigated via Shimadzu X-ray diffractometer (XRD-6000) with Cu-K α radiation and wavelength $\lambda = 1.541 \text{ \AA}$. Furthermore, the element composition analysis was observed by the energy dispersion X-ray spectrometer (Bruker X Flsh 6L10, EDX). The compact char surface (FT-IR) was distinguished using a Thermo Nicolet Nexus, ranging from 400 to 4,000 cm^{-1} . Finally, the topographical and the particle size features were studied using AFM (SPM AA3000-AFM) and EM10C TEM, respectively.

Antifungal and Antibacterial Activities

Using the well-known agar well diffusion technique,²⁶ CuO NPs antifungal activity was screened against two fungal strains namely *Candida* and *Aspergillus* species. Nutrient agar plates were thoroughly swabbed using sterile cotton swap with saturated 30 mL of 24 hours Sabouraud's dextrose agar culture media of each fungal strain. Wells were provided using cork borer (5 mm) in the pre-solidified agar plates. Different concentrations (25, 50, 100, 200, 400, and 800 $\mu\text{g/mL}$) of the synthesized CuO NPs, after sonicating for 30 minutes, were employed to assess the NPs antifungal activity. DDW

and standard antibiotics were negative and positive control against fungal pathogens, respectively. The antifungal used are Ketoconazole (KCA, 10 μg), Nystatin (NY, 100 μm), Amphotericin B (AMB, 20 μg), and Fluconazole (FCN, 10 μg). Afterward, plates were incubated for 48 hours at 35°C, and inhibition zones were measured in millimeters.

In a similar procedure to the antifungal activity, the antibacterial activity was monitored against gram-positive *S. aureus* and gram-negative *Asinobacterial spp.* using CuO NPs (25, 50, 100, and 200 $\mu\text{g/mL}$). However, 30 mL of 24 hours of blood agar culture media of each separate isolated bacterial species were used. DDW was used as a negative control and standard antibiotics as a positive control; antibiotics used were Cerftriaxone (CRO, 30 μg), Amikacin (AK, 30 μg), Ampicillin 10 μg , Sulbactam 10 μg (SAM, 20 μg), Trimethoprim (TS, 1.25 μg), Clindamycin (CD, 2 μg), Ciprofloxacin (CIP, 5 μg), and Azithromycin (ATH, 15 μg). Finally, the antibacterial activity was recorded after incubation for 24 hours at 35°C.

RESULTS AND DISCUSSION

Characterization of CuO NPs

The XRD patterns of the synthesized CuO NPs are shown in Figure 1a, which can be indexed to the single-phase structure of CuO (JCPDS: 80-1916).²⁷ It can be clearly noticed that there are no impurities perceived in the XRD results; this indicates the purity and high crystallinity of the green synthesized CuO NPs.² However, it can be clearly observed (Figure 1a) that increasing the precursor concentration from 7 to 10 mm resulted in an upsurge of the peaks' intensity of the resultant CuO NPs, while further increment (15 mm) showed a decrease in the intensity. This indicates a better crystal quality at 10 mm concentration. Furthermore, the crystallite size was calculated in accordance with the Debye-Scherrer's module.²⁸ The crystallite size of 7, 10, and 15 mm CuO NPs at $2\theta = 35.5$, was estimated to be 20, 38, and 21 nm, respectively. It is well-known that the crystal quality can be evaluated using the crystallite size, where the full width at half maximum (FWHM) is inversely proportional to the crystal size in accordance with Debye-Scherrer's module.²⁹ The results demonstrate an increase in the crystallite size as the concentration increases, which in turn indicates a better crystal quality of the prepared nanoparticles at 10 mm concentration (Figure 1b).

The FTIR spectrum of the synthesized CuO NPs (concentration of 10 mm) is demonstrated in Figure 2. The spectral peaks of the FTIR spectrum suggest the

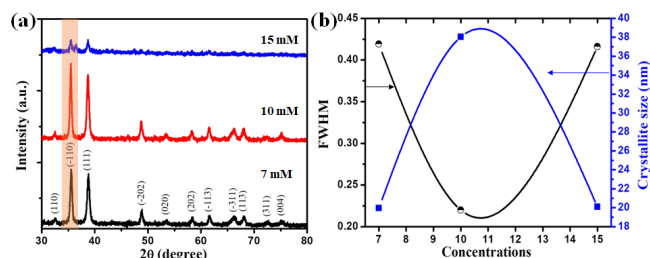


Figure 1: Structural properties of CuO NP; (a) XRD patterns, and (b) FWHM and crystallite size at $2\theta = 35.5$

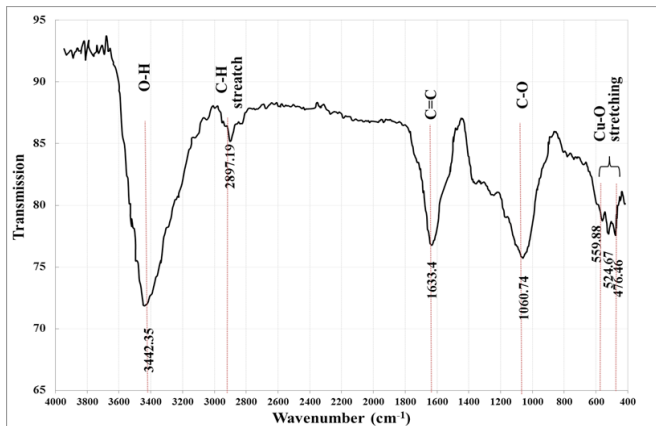


Figure 2: FTIR spectra of CuO NPs with 10 mm concentration

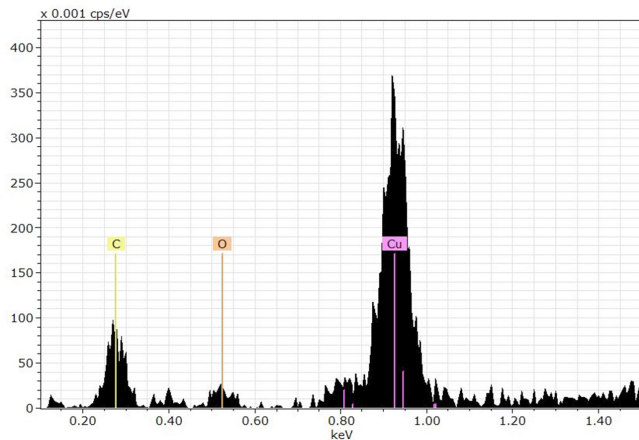


Figure 3: Energy dispersion X-ray spectra of CuO NPs

occurrence of O-H stretching ($3,442.35\text{ cm}^{-1}$), C-H stretching ($2,897.19\text{ cm}^{-1}$), C=C aromatic ($1,633.4\text{ cm}^{-1}$), and C-O stretching ($1,060.74\text{ cm}^{-1}$).³⁰ The presence of bands at 476.46 , 524.67 , and 559.88 cm^{-1} , corresponding to the vibrations of Cu-O, confirms the formation of CuO NPs.³¹

The purity and chemical composition of the prepared nanoparticles (10 mm) were investigated using the EDX technique, as illustrated in Figure 3. The weight percentage of both copper and oxide was calculated from the EDX outcomes, to be 3.56 and 75.14 weight%, respectively. Additionally, other elemental impurities, such as, the carbon in the EDX spectra was found to be 21.31 weight%.

Figure 4 reveals two- and three-dimensional images of CuO NP AFM outcomes with a concentration of 10 mm. As depicted in Figure 4, CuO NPs demonstrated a well-uniform disruption of spherical shape and grains with upfront alignment. The grain size was found to be 60.15 nm. It is generally known that nanoparticles with rough surface features provide a major role in electrochemical activity as compared to smooth ones.³² The values of root mean square (RMS) and surface roughness average was estimated to be 9.96 and 8.6 nm, which indicates a highly rough surface of the prepared CuO NPs.

The TEM image of CuO NPs is illustrated in Figures 5a and b. This study is carried out in order to develop a deep understanding of the crystalline characteristics of the

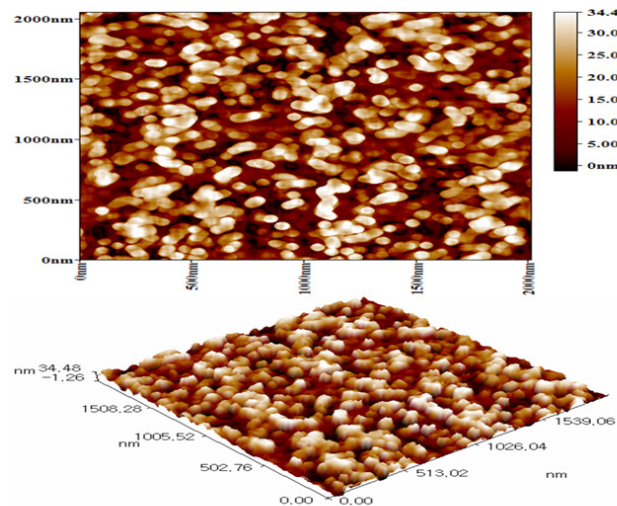


Figure 4: AFM images of green synthesized CuO NPs

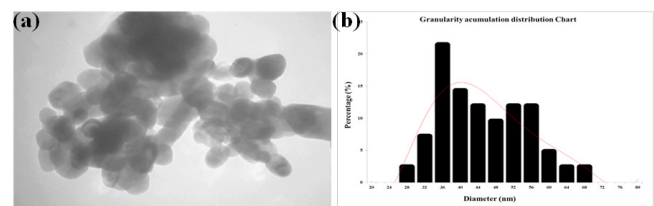
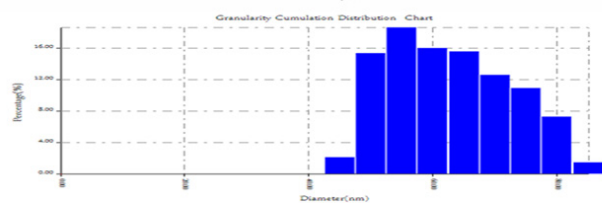


Figure 5: CuO NPs with 10 mm concentration; (a) TEM image; (b) Diameter range distribution

prepared 10 mm CuO NPs. In general (Figure 5a), the prepared nanoparticles exhibited a spherical shape with an approximately average diameter of $\sim 41.5\text{ nm}$. As shown in Figure 5b, a uniform nanoparticle distribution can be observed with a minimum and maximum percentage of nanoparticles diameters of 28 and 36 nm, respectively.

Antifungal Activity

It is generally known that the size of a bacterial cell typically ranges in a micrometer scale, where these cells contain membranes with nanometer range pores.³³ Therefore, nanoparticles, with a size range comparable to that of pore size, demonstrates the unique property of a clear passage to the cell membrane without exertion. This agrees well with the current study findings, as illustrated in the TEM analysis.

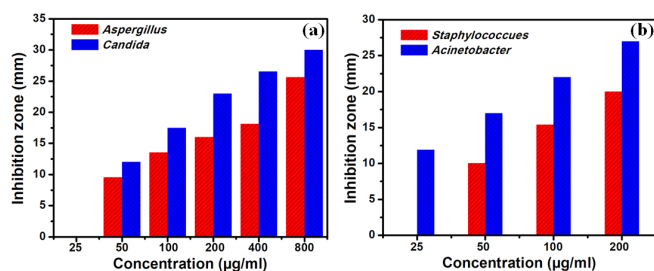
Antifungal activity of the CuO NPs on both strains, *Candida*, and *Aspergillus* species, are illustrated in Figure 6a, respectively. As demonstrated in Figure 6a, a substantial growth inhibition effect of fungal culture using CuO NPs was noticed with respect to the positive control. The antifungal activity in the case of *Candida* species indicated that $50\text{ }\mu\text{g/mL}$ concentration of CuO NPs inhibits fungal diameter progress of 12 mm, however, increasing CuO NPs concentration to

Table 1: Zone of inhibition diameters of antibiotics used against fungal isolates, CuO NPs, and DDW

Fungal	Minimum inhibition zone (mm)					
	KCA (10 µg)	NY (100 un)	AMB (20 µg)	FCN (10 µg)	DDW	CuO NPs
<i>Candida</i> spp.	35	16	11.4	25	0	11
<i>Aspergillus</i> spp.	21	16	12	0	0	10.6

Table 1: Zone of inhibition diameters of antibiotics used against bacterial isolates, CuO NPs, and DDW

Bacterial isolates	Minimum inhibition zone (mm)								
	CRO (30 µg)	AK (30 µg)	SAM (20 µg)	TS (25 µg)	CD (2 µg)	CIP (5 µg)	ATH (15 µg)	DDW	CuO NPs
<i>S. aureus</i>	25	18.2	17	15	0	0	0	0	9.75
<i>Acinetobacter baumannii</i>	0	0	0	0	0	0	0	0	12.2

**Figure 6:** Inhibition zones of CuO NPs for (a) fungi, and (b) bacteria

800 µL/mL, showed a higher diameter interval of 30 mm. In the event of *Aspergillus* species, inhibition zones of 9.5 and 25.7 mm were perceived for CuO NPs concentration of 50 and 800 µL/mL, respectively. The results specify that CuO NPs have a higher effect on *Candida* species, as compared to the case of *Aspergillus* species. From the aforementioned investigation, it can be clearly anticipated that the synthesized nanoparticles are operative in inhibiting/killing a noticeable diameter range of fungal growth, yet a higher concentration of CuO NPs is of great importance. A possible explanation could be the uninterrupted interaction between the external membrane surface of the fungal and the synthesized nanoparticles.³³

Antibacterial Activity

The antibacterial testing of the proposed study revealed that CuO NPs demonstrated a significant performance as antibacterial agents against both gram-positive *S. aureus* and gram-negative *Asinobacterial* species as presented in Figure 6b, respectively. Particularly, the diameter of the inhibition zone was found to be proportional to nanoparticle concentration in the medium. The effect of CuO NPs on gram-negative bacteria growth was found higher as compared to the effect on gram-positive bacteria. In detail, inhibition zone diameters were found to be 10 and 20 mm, as the concentration of the nanoparticles increased from 50 to 200 µg/mL, respectively, against gram-positive *S. aureus*. Whilst in the case of gram-negative *Asinobacterial*, diameters of the inhibition zones were found to be 17 and 27 mm, with nanoparticles concentration of 50 and 200 µL/mL, respectively. It is also noteworthy mentioning that CuO NPs exhibited effects on gram-negative *Asinobacterial*, with concentration as low as 25 µL/mL, while contrariwise, this behavior was

not noticed on gram-positive *S. aureus*. As demonstrated in Tables 1 and 2, the green synthesized CuO NPs demonstrated higher anti-bacterial and anti-fungal effects in comparison to the standard antibiotics.

In general analysis of both antifungal and antibacterial activities, it is clear to be noticed that CuO NPs inhibited higher zone diameter on fungi than bacteria with respect to the concentration of the nanomaterials.

CONCLUSION

The green synthesis of CuO NPs using POX enzyme fig leaves extract for antifungal and antibacterial activities was successfully outlined. Afterward, a comprehensive analysis of the prepared nanoparticles was demonstrated, by which CuO NPs with a diameter in the range of 28 to 68 nm were acquired. The antifungal activity was screened, using the synthesized CuO NPs, against *Candida* and *Aspergillus* species, while antibacterial activity was monitored on gram-positive *S. aureus* and gram-negative *Asinobacter baumannii*. It was proven that POX fig leaves extract plays a crucial role in elevating the effect of CuO NPs for both antifungal and antibacterial activities. It can be concluded that the green synthesized CuO NPs demonstrated a higher effect on the tested fungi compared to tested bacteria used in this study.

REFERENCES

- Gültekin DD, Güngör AA, Önem H, Babagil A, Nadaroğlu H. Synthesis of copper nanoparticles using a different method: determination of its antioxidant and antimicrobial activity. *Journal of the Turkish Chemical Society, Section A: Chemistry*. 2016;3(3):623-636.
- Naika HR, Lingaraju K, Manjunath K, Kumar D, Nagaraju G, Suresh D, Nagabhushana H. Green synthesis of CuO nanoparticles using *Gloriosa superba* L. extract and their antibacterial activity. *Journal of Taibah University for Science*. 2015 Jan 1;9(1):7-12.
- Yang S, Wang C, Chen L, Chen S. Facile dicyandiamide-mediated fabrication of well-defined CuO hollow microspheres and their catalytic application. *Materials Chemistry and Physics*. 2010 Apr 15;120(2-3):296-301.
- Umar A, Rahman MM, Al-Hajry A, Hahn YB. Enzymatic glucose biosensor based on flower-shaped copper oxide nanostructures composed of thin nanosheets. *Electrochemistry Communications*. 2009 Feb 1;11(2):278-281.

5. Salih EY, Sabri MF, Tan ST, Sulaiman K, Hussein MZ, Said SM, Yap CC. Preparation and characterization of ZnO/ZnAl₂O₄ mixed metal oxides for dye-sensitized photodetector using Zn/Al-layered double hydroxide as precursor. *Journal of Nanoparticle Research*. 2019 Mar 1;21(3):55.
6. Tamaki J, Shimanoe K, Yamada Y, Yamamoto Y, Miura N, Yamazoe N. Dilute hydrogen sulfide sensing properties of CuO–SnO₂ thin film prepared by low-pressure evaporation method. *Sensors and Actuators B: Chemical*. 1998 Jun 25;49(1-2):121-125.
7. Vijaya Kumar R, Elgamiel R, Diamant Y, Gedanken A, Norwig J. Sonochemical preparation and characterization of nanocrystalline copper oxide embedded in poly (vinyl alcohol) and its effect on crystal growth of copper oxide. *Langmuir*. 2001 Mar 6;17(5):1406-1410.
8. Bashir MB, Said SM, Sabri MF, Miyazaki Y, Shnawah DA, Shimada M, Salleh MF, Mahmood MS, Salih EY, Fitriani F, Elsheikh MH. In-Filled La_{0.5}Co₄Sb₁₂ Skutterudite System with High Thermoelectric Figure of Merit. *Journal of Electronic Materials*. 2018 Apr 1;47(4):2429-2438.
9. Bashir MB, Sabri MF, Said SM, Miyazaki Y, Badruddin IA, Shnawah DA, Salih EY, Abushousha S, Elsheikh MH. Enhancement of thermoelectric properties of Co₄Sb₁₂ Skutterudite by Al and La double filling. *Journal of Solid State Chemistry*. 2020 Apr 1;284:121-205.
10. Yip SK, Sauls JA. Nonlinear Meissner effect in CuO superconductors. *Physical review letters*. 1992 Oct 12;69(15):2264.
11. Grigore ME, Biscu ER, Holban AM, Gestal MC, Grumezescu AM. Methods of synthesis, properties and biomedical applications of CuO nanoparticles. *Pharmaceuticals*. 2016 Dec;9(4):75.
12. Carnes CL, Stipp J, Klabunde KJ, Bonevich J. Synthesis, characterization, and adsorption studies of nanocrystalline copper oxide and nickel oxide. *Langmuir*. 2002 Feb 19;18(4):1352-1359.
13. Wang H, Xu JZ, Zhu JJ, Chen HY. Preparation of CuO nanoparticles by microwave irradiation. *Journal of crystal growth*. 2002 Sep 1;244(1):88-94.
14. Yin AJ, Li J, Jian W, Bennett AJ, Xu JM. Fabrication of highly ordered metallic nanowire arrays by electrodeposition. *Applied Physics Letters*. 2001 Aug 13;79(7):1039-1041.
15. Xu JF, Ji W, Shen ZX, Tang SH, Ye XR, Jia DZ, Xin XQ. Preparation and characterization of CuO nanocrystals. *Journal of Solid State Chemistry*. 1999 Nov 1;147(2):516-519.
16. Fan H, Yang L, Hua W, Wu X, Wu Z, Xie S, Zou B. Controlled synthesis of monodispersed CuO nanocrystals. *Nanotechnology*. 2003 Nov 10;15(1):37.
17. Xu, C., Liu, Y., Xu, G. and Wang, G., 2002. Preparation and characterization of CuO nanorods by thermal decomposition of CuC₂O₄ precursor. *Materials Research Bulletin*, 37(14), pp.2365-2372.
18. Shankar SS, Rai A, Ankamwar B, Singh A, Ahmad A, Sastry M. Biological synthesis of triangular gold nanoprisms. *Nature materials*. 2004 Jul;3(7):482-488.
19. Gardea-Torresdey JL, Gomez E, Peralta-Videa JR, Parsons JG, Troiani H, Jose-Yacamán M. Alfalfa sprouts: a natural source for the synthesis of silver nanoparticles. *Langmuir*. 2003 Feb 18;19(4):1357-1361.
20. Ravikumar BS, Nagabhushana H, Sunitha DV, Sharma SC, Nagabhushana BM, Shivakumara C. Plant latex mediated green synthesis of ZnAl₂O₄: Dy³⁺ (1–9 mol%) nanophosphor for white light generation. *Journal of alloys and compounds*. 2014 Feb 5;585:561-571.
21. Ankamwar B, Chaudhary M, Sastry M. Gold nanotriangles biologically synthesized using tamarind leaf extract and potential application in vapor sensing. *Synthesis and Reactivity in Inorganic, Metal-Organic and Nano-Metal Chemistry*. 2005 Jan 1;35(1):19-26.
22. Huang J, Li Q, Sun D, Lu Y, Su Y, Yang X, Wang H, Wang Y, Shao W, He N, Hong J. Biosynthesis of silver and gold nanoparticles by novel sundried Cinnamomum camphora leaf. *Nanotechnology*. 2007 Feb 6;18(10):105104.
23. Hu J. Biosynthesis of SnO₂ nanoparticles by Fig (*Ficus carica*) leaf extract for electrochemically determining Hg (II) in water samples. *Int. J. Electrochem. Sci*. 2015 Dec 1;10(12):10668-10676.
24. Cicek S, Gungor AA, Adiguzel A, Nadaroglu H. Biochemical evaluation and green synthesis of nano silver using peroxidase from *Euphorbia* (*Euphorbia amygdaloides*) and its antibacterial activity. *Journal of Chemistry*. 2015 Jan 1;2015.
25. Varghese D, Tom C, and Krishna N. Effect of CTAB on structural and optical properties of CuO nanoparticles prepared by coprecipitation route. in *Materials Science and Engineering Conference Series*. 2017;12:122-111.
26. Pérez Rodríguez C. An Antibiotic assay by the agar well diffusion method. 2018;1:22-34.
27. Shanan ZJ, Hadi SM, Shanshool SK. Structural analysis of chemical and green synthesis of CuO nanoparticles and their effect on biofilm formation. *Baghdad Science Journal*. 2018;15(2):211-216.
28. Salih EY, Sabri MF, Hussein MZ, Sulaiman K, Said SM, Saifullah B, Bashir MB. Structural, optical and electrical properties of ZnO/ZnAl₂O₄ nanocomposites prepared via thermal reduction approach. *Journal of Materials Science*. 2018 Jan 1;53(1):581-590.
29. Salih EY, Sabri MF, Sulaiman K, Hussein MZ, Said SM, Usop R, Salleh MF, Bashir MB. Thermal, structural, textural and optical properties of ZnO/ZnAl₂O₄ mixed metal oxide-based Zn/Al layered double hydroxide. *Materials Research Express*. 2018 Sep 5;5(11):116202.
30. Sankar R, Maheswari R, Karthik S, Shivashangari KS, Ravikumar V. Anticancer activity of *Ficus religiosa* engineered copper oxide nanoparticles. *Materials Science and Engineering: C*. 2014 Nov 1;44:234-239.
31. Sankar R, Manikandan P, Malarvizhi V, Fathima T, Shivashangari KS, Ravikumar V. Green synthesis of colloidal copper oxide nanoparticles using *Carica papaya* and its application in photocatalytic dye degradation. *Spectrochimica Acta Part A: Molecular and Biomolecular Spectroscopy*. 2014 Mar 5;121:746-750.
32. Soomro RA, Sherazi SH, Memon N, Shah MR, Kalwar NH, Hallam KR, Shah A. Synthesis of air stable copper nanoparticles and their use in catalysis. *Adv. Mater. Lett*. 2014;5(4):191-198.
33. Jadhav S, Gaikwad S, Nimse M, Rajbhoj A. Copper oxide nanoparticles: synthesis, characterization and their antibacterial activity. *Journal of Cluster Science*. 2011 Jun 1;22(2):121-129.